Prostaglandin F2α Agonists Negatively Modulate the Size of 3D Organoids from Primary Human Orbital Fibroblasts

Kaku Itoh, Fumihito Hikage, Yosuke Ida, and Hiroshi Ohguro

Department of Ophthalmology, Sapporo Medical University School of Medicine, Sapporo, Japan

Correspondence: Fumihito Hikage, Sapporo Medical University School of Medicine, 17 Chome Minami 1 Jonishi, Chuo Ward, Sapporo, Hokkaido 060-8556, Japan; fuhika@gmail.com.

KI and FH contributed equally to the work presented here and therefore should be regarded as equivalent authors.

Received: January 27, 2020
Accepted: May 3, 2020
Published: June 5, 2020

Citation: Itoh K, Hikage F, Ida Y, Ohguro H. Prostaglandin F2α agonists negatively modulate the size of 3D organoids from primary human orbital fibroblasts. *Invest Ophthalmol Vis Sci.* 2020;61(6):13. https://doi.org/10.1167/iovs.61.6.13

Purpose. To elucidate the molecular etiology of deepening of the upper eyelid sulcus (DUES) induced by prostaglandin (PG) analogs, a three-dimensional (3D) tissue culture system was employed using human orbital fibroblasts (HOFs).

Methods. During adipogenesis, changes in HOF 3D organoid sizes, as well as their lipids stained by BODIPY and expression of the extracellular matrix (ECM) by immunolabeling and/or quantitative PCR, were studied in the presence or absence of either 100-nM bimatoprost acid or 100-nM prostaglandin F2α.

Results. The size of the 3D organoids increased remarkably during adipogenesis, but such increases were significantly inhibited by the presence of PG analogs. Staining intensities by BODIPY and mRNA expression of peroxisome proliferator-activated receptor gamma were significantly increased upon adipogenesis but were not influenced by the presence of PG analogs. Unique changes in ECM expression observed with or without adipogenic differentiation were significantly modified by the presence of PG analogs.

Conclusions. Our present study indicates that PG analogs have the potential to modulate the ECM network within HOF 3D organoids. Thus, a 3D tissue culture system may be a suitable strategy for understanding the disease etiology of DUES.

Keywords: deepening of the upper eyelid sulcus, prostaglandin analogs, three-dimensional tissue culture

Glaucomatous optic neuropathy (GON) is known as a progressive and chronic optic neuropathy that may lead to irreversible blindness.[1,2] Several factors are known to be involved in GON, including direct damage of axons, microvascular failure, genetic factors, structural failure from myopic changes, and autoimmunity.[3–5] Among these factors, intraocular pressure (IOP) is believed to be the most important risk factor for the progression of GON; therefore, lowering IOP by anti-glaucoma medication, laser treatment, or surgery is the only evidence-based, effective treatment for GON.[6–9]

Among anti-glaucoma medications, prostaglandin (PG) analogs have been approved as first-line drugs. They are believed to be highly effective at lowering IOP through the prostanoid F-type prostaglandin (FP) receptor, maintaining vision for a longer period without any serious systemic side-effects.[10–12] Recently, however, longer use of PG analogs has resulted in local side effects recognized as prostaglandin-associated periorbitopathy, including conjunctival injection, hyperpigmentation of iris and skin, elongation of eyelashes, and deepening of the upper eyelid sulcus (DUES).[13–15]

DUES has been reported as a cosmetic side effect of PG analogs, such as bimatoprost (BIM), travoprost, tafluprost, and latanoprost.[16–19] Among these drugs, BIM and travoprost are particularly known to increase the risk of DUES.[17,20] Inoue et al.[21] reported that the incidence of DUES was 60.0% in patients using BIM, 50.0% with travoprost, 24.0% with latanoprost, and 18.0% with tafluprost. As a possible mechanism of DUES, it has been suggested that orbital fat atrophy, which can be observed by using magnetic resonance imaging and histological analysis, is involved.[22]

Adipocytes are known to be involved in the control of energy homeostasis by regulating the fat storage and mobilization of free fatty acids in response to a variety of nutritional and hormonal conditions.[23] Adipogenesis requires the differentiation of preadipocytes into mature adipocytes by transcriptional programs regulating specific adipogenic genes.[24,25] With regard to the relationship between PG analogs and adipogenesis, it has been reported that PG analogs suppress adipogenesis through activation of the FP receptor.[26] Moreover, the use of a conventional two-dimensional (2D) tissue culture system has demonstrated that PG analogs can inhibit preadipocyte differentiation by downregulating the expression of adipogenic transcription factors, including peroxisome proliferator-activated receptor gamma (PPARγ).[27] Although such a 2D cell culture system is a major technique for cell culture and suited for evaluating cell–matrix interactions, it is difficult to characterize some properties of tissues, such as their relationships with the network of extracellular matrices (ECMs), within a three-dimensional (3D) space.[28] Some studies have reported that cell behavior is altered notably when cells are embedded within a 3D matrix in contrast with the cell–matrix interactions seen in 2D cultures.[29,30] Thus, the 3D tissue culture system has emerged as a novel ex vivo approach to modeling many diseases,[31,32] and the recently developed 3D organoid

culture system appears to be more suitable for identifying the mechanisms within adipogenesis that are involved in the etiology of DUES caused by PG analogs. In addition, several studies have suggested that physiological properties of orbital fatty tissues may be different from those of 3T3-L1 cells.[33] Thus, human orbital fibroblasts (HOFs) rather than 3T3-L1 cells should be desirable for this purpose.

The purpose of the current study was to establish a DUES cell model based on a 3D culture system using HOFs obtained from human orbital fat tissues and to examine the effects of PG analogs on the size of 3D organoids and ECM expression within the organoid during their adipogenesis.

Materials and Methods

This study was conducted at Sapporo Medical University Hospital, Japan, after approval by the institutional review board and according to the tenets of the Declaration of Helsinki and national laws for the protection of personal data. Informed consent was obtained from all participants in the study.

Human Orbital Fibroblast Isolation and Culture

HOFs were collected as surgical waste specimens of herniated orbital fat from four patients. Explants were cut and divided into small pieces, placed on 100-mm culture dishes, and completely submerged in a growth medium composed of Dulbecco's Modified Eagle Medium supplemented with 10% fetal bovine serum, 1% L-glutamine, and 1 % Antibiotic-Antimycotic (Thermo Fisher Scientific, Waltham, MA, USA). They were subsequently grown in a humid incubator at 37°C with 5% CO_2, and the medium was changed at 2- or 3-day intervals. HOFs used for all experiments described below were prepared during three to seven passages after the initial cell isolation.

3D Cell Culture and Adipogenic Differentiation of HOFs

HOF cells prepared as above were cultured in 100-mm or 150-mm dishes until reaching 90% to 100% confluence, washed with PBS twice, detached by 0.25% trypsin-EDTA, resuspended with a growth medium, and centrifuged at 300×*g* for 5 minutes. 3D organoid preparations were carried out on hanging drop culture plates (HDP1385; Sigma-Aldrich, St. Louis, MO, USA) as described recently.[32] Briefly, the cell pellet obtained as above was resuspended in a growth medium containing 0.25% METHOCEL (DuPont Nutrition & Biosciences, Copenhagen, Denmark) to stimulate morphological stability. Approximately 20,000 cells in a 28-µL drop were placed in each well of a hanging drop culture plate (day 0). Thereafter, 14 µL of the culture medium was removed and a fresh 14 µL of the culture medium was added to each well every day until day 12 for HOFs. During the course of the 3D culture, HOFs grew into a sphenoid-shaped organoid. Adipogenic differentiation of HOFs was induced by a cocktail containing 250-nM dexamethasone, 10-nM T3, 10 µg/ml insulin, and 10-mM troglitazone from day 1 through day 5. This was followed by the use of a cocktail containing 10 µg/ml insulin and 10-mM troglitazone from day 6 through day 11 for HOFs in the presence or absence of 100-µM BIM or 100-µM prostaglandin F2α (PGF2α). 3D cell organoids of HOFs at day 12 were collected for RNA preparation or immunostaining. As a control, 3D culture cells were treated as above in the growth medium containing 0.1% dimethyl sulfoxide without the adipogenic stimulation.

Measurement and Evaluation of 3D Organoid Sizes

Bright-field images of organoids were captured in a 4× objective lens using an inverted microscope (Nikon ECLIPSE Ts2; Tokyo, Japan). For evaluation of each organoid size, the largest cross-sectional area was measured using Image J 1.51n (National Institutes of Health, Bethesda, MD, USA).

Gene Expression Analysis

Total RNA was extracted from 16 organoids using an RNeasy mini kit (Qiagen, Hilden, Germany). Reverse transcription was performed with the SuperScript IV kit (Invitrogen, Carlsbad, CA, USA) in accordance with the manufacturer's instruction. Respective gene expression was quantified by real-time PCR with either Power SYBR Green or Universal TaqMan Master Mix and the Applied Biosystems StepOnePlus system (Thermo Fisher Scientific). cDNA quantities were normalized to the expression of housekeeping gene 36B4 (RPLP0) and are shown as fold changes relative to the control. DNA sequences of primers and TaqMan probes were as follows:

- Human RPLP0: probe, 5′-/56-FAM/CCCTGTCTT/ZEN/CCCTGGGCATCAC/3IABkFQ/-3′; forward, 5′-TCGTCTTTAAACCCTGCGTG-3′; reverse, 5′-TGTCTGCTCCCACAATGAAAC-3′
- Human COL-1A1: probe, 5′-/56-FAM/TCCAGGGCC/ZEN/AAGACGAAGACATC/3IABkFQ/-3′; forward, 5′-GACATGTTCAGCTTTGTGGAC-3′; reverse, 5′-TTCTGTACGCAGGTGATTGG-3′
- Human COL-4A1: probe, 5′-/56-FAM/TCATACAGA/ZEN/CTTGGCAGCGGCT/3IABkFQ/-3′; forward, 5′-AGAGAGGAGCGAGATGTTCA-3′; reverse, 5′-TGAGTCAGGCTTCATTATGTTCT-3′
- Human COL-6A1: forward, 5′-CCTCGTGGACAAAGTCAAGT-3′; reverse, 5′-GTGAGGCCTTGGATGATCTC-3′
- Human FN-1: forward, 5′-CGTCCTAAAGACTCCATGATCTG-3′; reverse, 5′-ACCAATCTTGTAGGACTGACC-3′

Immunofluorescent Labeling of 3D Organoids

3D cultured organoids were fixed in 4% paraformaldehyde in PBS overnight without permeabilization. After blocking in 3% BSA in PBS for 3 hours at room temperature, organoids were washed twice with PBS for 20 minutes. Samples were then incubated with a primary antibody (1:200 dilutions) including anti-collagen type 1 (COL-1), type 4 (COL-4), or type 6 (COL-6) or anti-fibronectin-1 (FN-1) at 4°C overnight. Thereafter, samples were washed three times with PBS for 60 minutes, followed by incubation with Invitrogen Goat anti-Rabbit IgG (H+L) Cross-Adsorbed Secondary Antibody, Alexa Fluor 488, for collagens, or Goat anti-Mouse IgG (H+L) Highly Cross-Adsorbed Secondary Antibody, Alexa Fluor Plus 488, for fibronectin (1:500 dilution), as well as phalloidin and 4′,6-diamidino-2-phenylindole (DAPI) (1:1000 dilution), for 3 hours at room temperature. Alternatively, for lipid staining, samples were incubated with BODIPY FL dye (Thermo Fisher Scientific), phalloidin, and DAPI

Investigative Ophthalmology & Visual Science

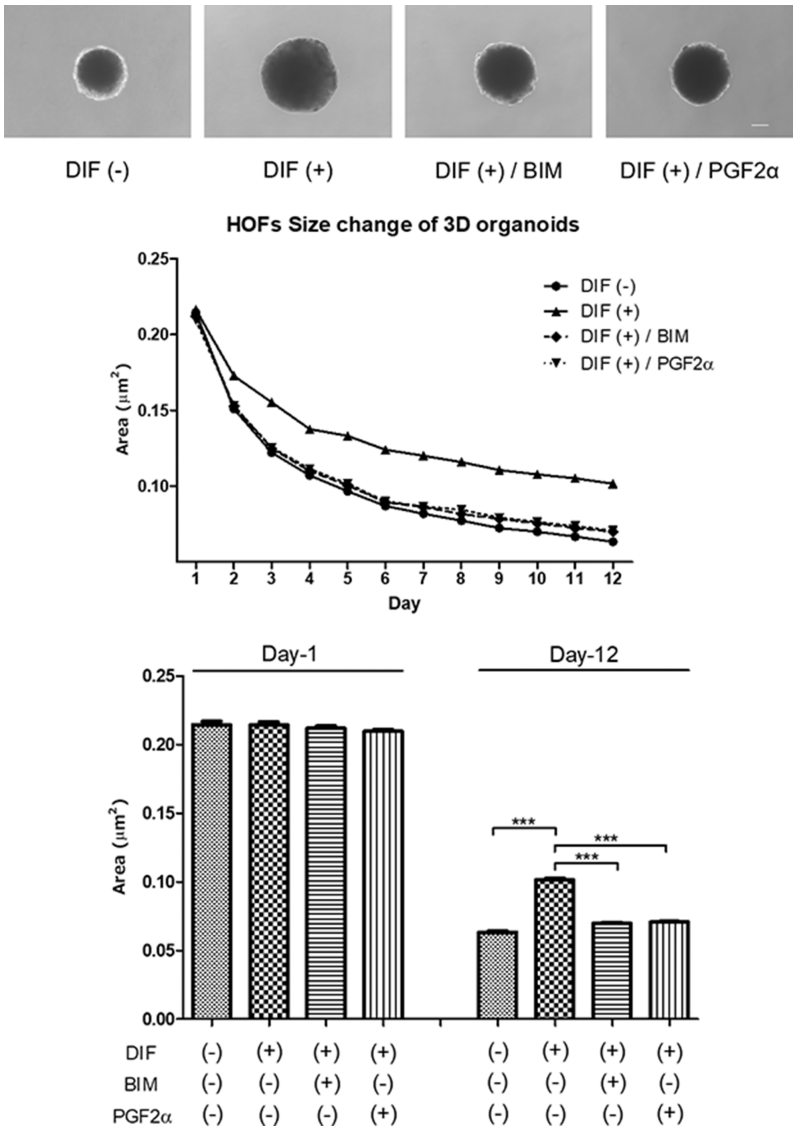

Figure 1. Representative images of HOF organoids (*top*), and changes in their sizes during the 3D cell culture in the presence or absence of PG analogs (*middle* and *bottom*). Representative phase contrast images of four groups of 3D culture at day 12 consist of (1) organoids of HOF preadipocytes as control (DIF–), (2) their differentiation (DIF+), (3) DIF+ in the presence of 100-nM bimatoprost free acid (DIF+/BIM), and (4) DIF+ in the presence of 100-nM prostaglandin F2α (DIF+/PGF2α). *Scale bar*: 100 μm (*top*). Changes in mean sizes of the 3D organoids in each condition were plotted for the 3D cultures until day 12 (*middle*), and those at day 1 and day 12 were compared among groups (*bottom*). The mean sizes of organoids gradually became smaller and reached constant levels in each group. These levels significantly increased through the adipogenic differentiation (DIF+) as compared to that of preadipocytes (DIF–). Such effects of the organoid size were suppressed in the presence of BIM and PGF2α. All experiments were performed in duplicate using fresh preparations consisting of five organoids each. Data are presented as arithmetic mean ± SEM. $^{****}P < 0.001$ (ANOVA followed by a Tukey's multiple comparison test).

(1:1000 dilution) for 3 hours. These samples were then transferred on to a cover glass and mounted in ProLong Gold Antifade Mountant (Thermo Fisher Scientific). Immunofluorescent images were obtained using Nikon A1 confocal microscopy and NIS-Elements 4.0 software. Images of 2D cells were acquired with ×20 air objective lens with a resolution of 1024 × 1024 pixels. For images of 3D organoids, serial-axis imaging (2.2-μm intervals) 35 μm from the surface of organoids was conducted using a ×20 air objective lens with a resolution of 1024 × 1024 pixels; the images were converted into Z-stack images using the maximum intensity projection feature of the NIS-Elements 4.0 software. Among these Z-stack images, an image 20 μm from the bottom was used as a cross-sectional image. The intensity of immunofluorescent target proteins was quantified using ImageJ. The signal intensity of the organoids was expressed as the maximum intensity/surface area measured at 35 μm from the top of the organoid in the *z*-plane. The surface area was calculated as follows: surface area = $D \times A/(A + \pi \times H^2)$, where D indicates organoid diameter (μm), A indicates area of sectioned organoid (μm^2), and H indicates height (= 35 μm).

Statistical Analysis

All statistical analyses were performed using GraphPad Prism 7 (GraphPad Software, San Diego, CA, USA). One-way ANOVA was used to analyze the difference among matched

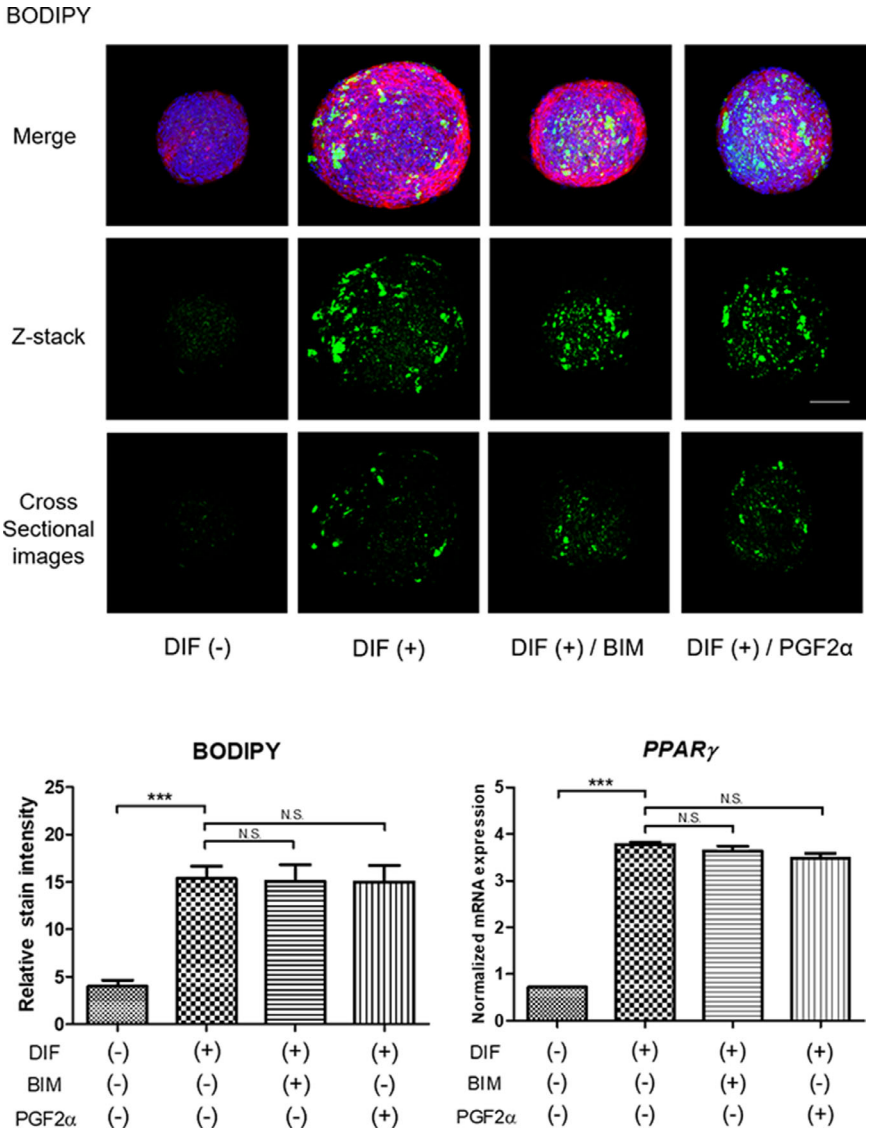

Figure 2. Confocal immunostaining images by lipid staining (BODIPY), phalloidin, and DAPI of preadipocytes (DIF–) or adipogenic (DIF+) HOF organoids (*top*), their intensities (*bottom left*), and mRNAs of PPARγ (*bottom right*) in the presence or absence of PG analogs. At day 12, 3D organoids were immunostained by BODIPY (*green*), DAPI (*blue*), or phalloidin (*red*). Their confocal merged image (*upper*) and Z-stack (*middle*) and cross-sectional images of BODIPY are shown in the top panels. *Scale bar*: 100 µm. Only a faint staining by BODIPY was observed in the organoid of HOF preadipocytes (DIF–). Through adipogenic differentiation, the staining intensities of both Z-stack and cross-sectional images were significantly enhanced (DIF+) in the presence or absence of BIM and PGF2α (*top* and *bottom left*). The gene expression of *PPARγ*, a master regulatory gene of the adipocyte differentiation, was also significantly increased by the adipogenic differentiation but was not influenced by BIM or PGF2α (bottom right). All experiments were performed in duplicate using fresh preparations consisting of five organoids each. Data are presented as arithmetic mean ± SEM. $^{***}P < 0.005$ (ANOVA followed by a Tukey's multiple comparison test).

multiple group comparisons, followed by a Tukey's multiple comparison test. Data are presented as arithmetic mean ± SEM.

Results

As shown in Figure 1 (top), uniform spheroidal 3D organoids were successfully generated from 20,000 HOF cells on a hanging drop culture system. They gradually diminished in size until reaching a steady state by day 12 (Fig. 1, middle). Upon adipogenic differentiation (DIF+), the 3D HOF organoid sizes increased markedly as compared to those without adipogenesis (DIF–) (Fig. 1, middle and bottom). With regard to the effects of PG analogs on the 3D HOF organoids, both 100-nM BIM and 100-nM PGF2α caused marked reduction in the adipogenesis-induced enlargement of their sizes (Fig. 1, middle and bottom).

To investigate the types of mechanisms involved in terms of the effects of PG analogs on HOF organoid growth during adipogenic differentiation, lipids stained by BODIPY and the gene expression of PPARγ, a molecular marker of the adipogenesis, were analyzed. Both relative intensities of lipids stained by BODIPY (Fig. 2, top and bottom left) and mRNA expression of PPARγ of the HOF organoids (Fig. 2, bottom right) were significantly increased by the adipogenic differentiation, whereas these changes were not altered by the presence of PG analogs. These observations suggest that factors other than lipid metabolism during adipogenesis

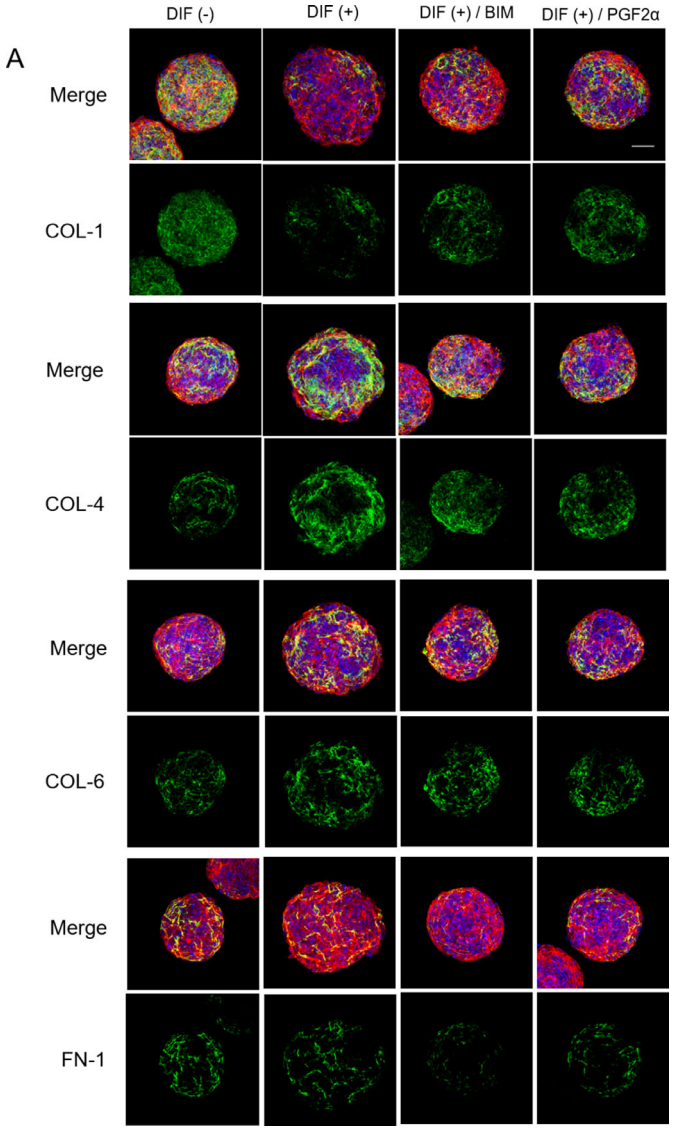

Figure 3. Confocal images of expressions of ECMs in 3D HOF organoids. At day 12, 3D organoids were immunostained by ECMs of COL-1, COL-4, COL-6, or FN-1 (*green*); DAPI (*blue*); or phalloidin (*red*). Confocal merged and immunostained images for each ECM antibody are shown in **A**. Experimental conditions were composed of 3D organoids of HOF preadipocytes as the control (DIF–) and their differentiation (DIF+) in the absence or presence of 100-nM bimatoprost free acid or 100-nM PGF2α. *Scale bar*: 100 µm. Staining intensities of ECMs as above are plotted in **B** (see top of next page). All experiments were performed in duplicate using fresh preparations consisting of five organoids each. Data are presented as arithmetic mean ± SEM. $^{*}P < 0.05$, $^{**}P < 0.01$, $^{***}P < 0.005$ (ANOVA followed by a Tukey's multiple comparison test).

could be involved in the mechanisms resulting in the smaller size of HOF organoids induced by PG analogs.

Next, to study the effects of PG analogs on the expression of major ECMs in HOFs, 3D organoids, including COL-1, COL-4, COL-6, and FN-1, were examined by immunofluorescent staining (Fig. 3) and mRNA expression (Fig. 4). The relative intensities of immunostaining of COL-1 and FN-1 were significantly reduced; in contrast, those of COL-4 and COL-6 were increased markedly by adipogenesis (Fig. 3). The presence of PG analogs suppressed these effects in COL-1 and COL-6 or increased them slightly in FN-1, but no effects were observed in COL-4 (Fig. 3). mRNA expression analysis supported such adipogenesis-induced changes and their modulations by PG analogs in the expression of ECMs (Fig. 4). Based on these results, we speculate that PG analogs may act as modulators of adipogenesis-induced ECM expression within HOFs, whereas, in contrast, lipid metabolism may have a small effect on the diminished size of the organoids caused by PG analogs.

Discussion

Recent studies have reported that one of the mechanisms of DUES is suppression of adipogenesis in orbital fat tissues after treatment with PG analogs, such that the expression of PPARγ is downregulated and adipogenesis is inhibited in both premature and mature adipocytes by PG analogs using a 2D culture system.[27] In terms of effects of anti-glaucoma medications on adipocytes, it was reported that PG analogs, including BIM, travoprost, latanoprost, and tafluprost, suppress preadipocyte proliferation, whereas timolol and benzalkonium chloride show significant

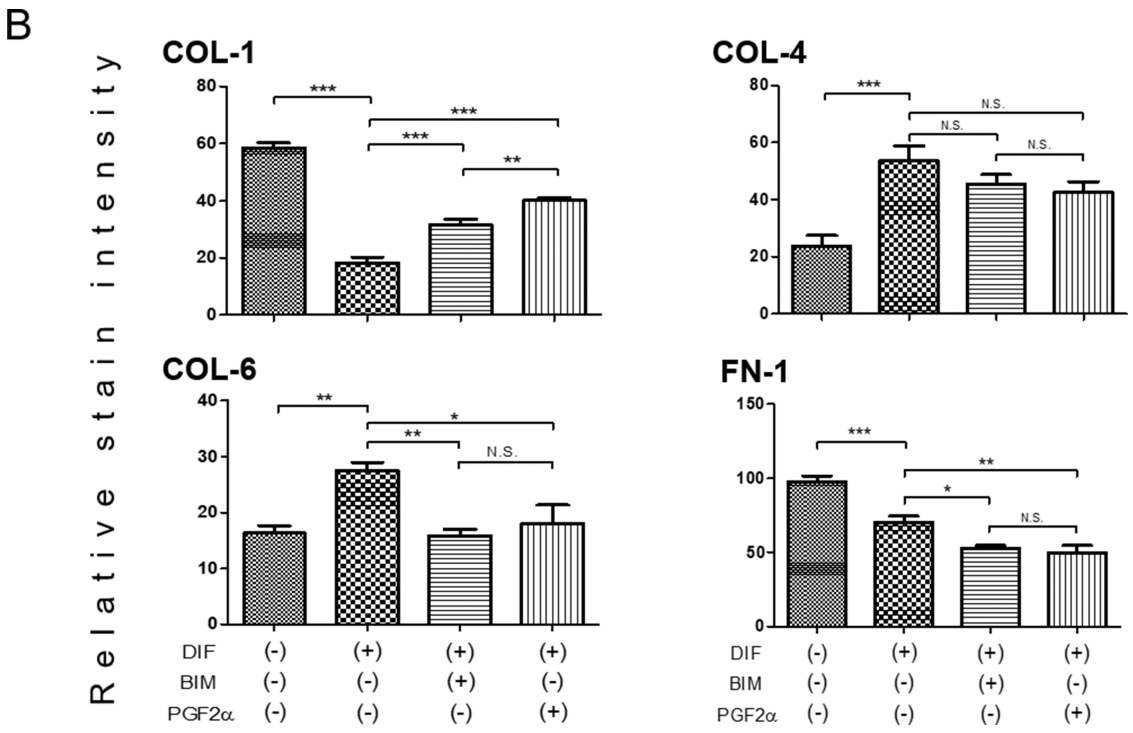

Figure 3. continued.

antiproliferative and cytotoxic effects toward adipocytes.[27,34] It is well known that BIM is an acid form of prostaglandin-type PG analogs derived from PGF2α by the addition of a phenyl base at C-17 and conservation of the C-15 hydroxyl base.[26,35] This is important for binding to the prostanoid FP receptor. As such, the effects of PG analogs toward adipocytes, thought to be involved in the etiology of DUES, may exclusively be mediated by the FP receptor. In fact, it has recently been determined, through FP receptor stimulation using a 2D 3T3-L1 culture and FP receptor knockout mice, that prostaglandin-type PG analogs inhibit adipogenesis.[26] Alternatively, it has been reported that BIM also inhibits adipogenesis of the orbital adipose-derived stem cells obtained from patients with thyroid-associated orbitopathy (TAO), suggesting that the PGF2α agonist might be a therapeutic candidate for the treatment of TAO.[36,37]

The 3D organoid culture system has recently received attention regarding how it may structure the model of many diseases through an ex vivo approach.[31] When compared to the 2D system, this method is more advantageous to evaluate the structure of tissues close to the biological context and network of ECM proteins.[30] However, one disadvantage of the system is its inability to determine the quantity of protein because of the smaller amounts of cells included in organoids. Our group recently utilized this 3D culture model with HOF cells for patients with TAO and found that HIF2A played a critical role in mediating lysyl oxidase-dependent ECM accumulation.[32] In a recent study (submitted for publication), we examined the effects of PG analogs on the adipogenesis of 3T3-L1 3D cell cultures and found that PG analogs, BIM, and PGF2α significantly suppressed the increase in organoid size, lipid contents, lipid laden structure, and gene expressions of PPARγ, in addition to affecting the spatial localization and distribution of ECMs within the 3D organoids during their adipogenic differentiation. This finding suggested that 3D cell culture is suitable to investigate the molecular etiology of DUES. In the present study, to identify further the effects of PG analogs on 3D organoids obtained from HOFs, we observed the following: Upon adipogenic differentiation, 3D organoids of HOFs became significantly bigger, but such changes were markedly suppressed by the presence of PG analogs. Levels of both lipids stained by BODIPY and mRNA expression of PPARγ were significantly enhanced by adipogenesis but were not affected by PG analogs. Finally, unique changes in ECM expression, decreases in COL-1 and FN-1, and an increase in COL-6 expression were observed upon adipogenesis, and the changes in COL-1 and COL-6 or in FN-1 were significantly suppressed or enhanced by the presence of PG analogs.

These observations suggest that, with regard to the molecular etiology of DUES, a factor other than suppression of adipogenesis might be involved in the volume loss of orbital fat tissues, presumably modulation of the ECM network. To confirm this speculation, we studied the effects of PG analogs on HOF organoids without induction of adipogenesis. The organoids were smaller during the course of the 3D culture of HOFs during day 12, and such changes were enhanced by the presence of PG analogs. In terms of ECM expression within their 3D organoids, PG analogs caused similar changes of ECMs as above, but these changes were smaller than for adipogenesis (data not shown).

ECM is an important multifunctional molecular group that provides structural support to organs, modifies cell–cell signals, and regulates various cellular functions.[38] Collagens are triple helical proteins that occur in the ECM and at the cell–ECM interface.[39] There are more than 30 COLs and COL-related proteins, but the most abundant is COL-1.[40,41] It is well known that COL-4 is a main component of the basement membrane ECM that surrounds each adipocyte.[42,43]

Investigative Ophthalmology & Visual Science

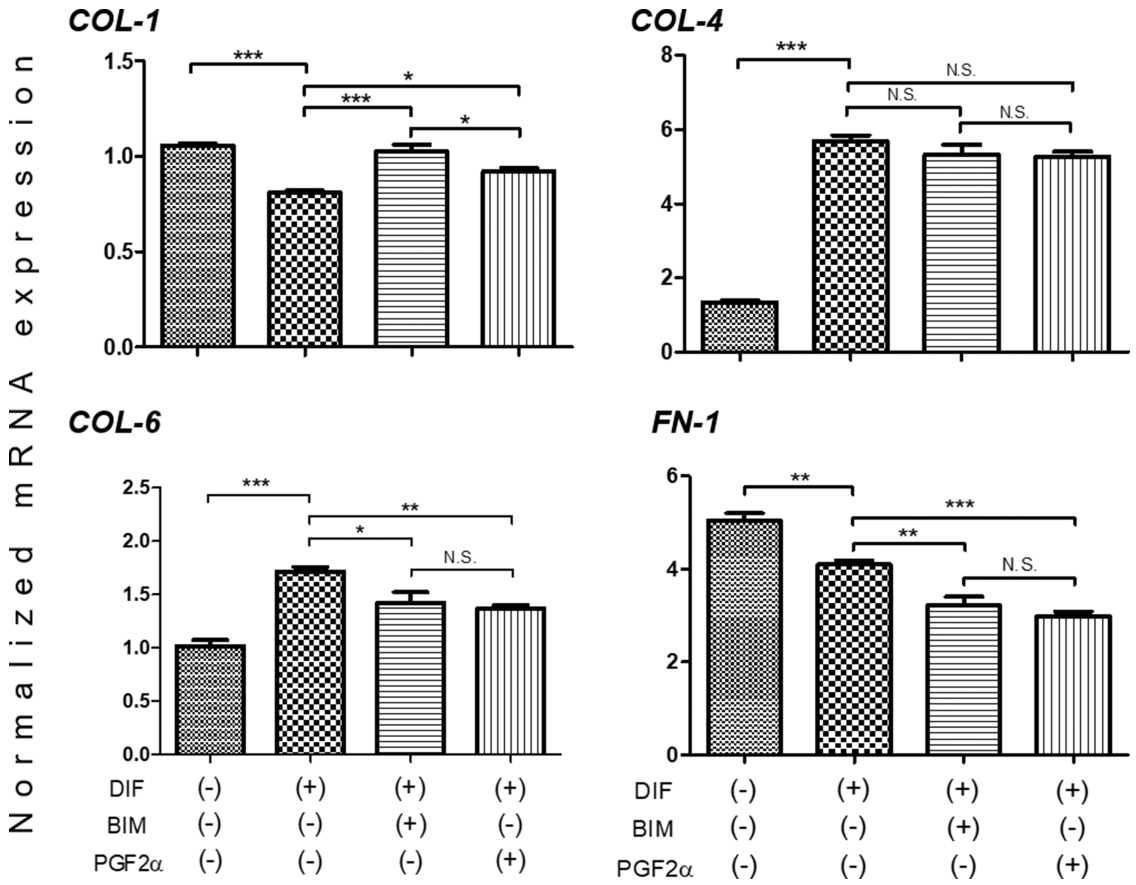

Figure 4. qPCR analyses of gene expressions of ECMs in 3D HOF organoids. At day 12, 3D culture organoids of HOFs preadipocytes as the control (DIF–) and their differentiation (DIF+) in the absence or presence of 100-nM bimatoprost free acid or 100-nM PGF2α were subjected to qPCR analysis to estimate mRNA expression of ECMs. All experiments were performed in duplicate using fresh preparations consisting of five organoids each. Data are presented as arithmetic mean ± SEM. $^{*}P < 0.05$, $^{**}P < 0.01$ (ANOVA followed by a Tukey's multiple comparison test).

COL-6, which forms microfibrils in the interface between the basement membrane and thick bundles of COL-1, is a major ECM that has important roles in the functions of several tissues and helps maintain the stemness and differentiation of many cell types.[44] In addition, COL-6 is also supposed to be a pivotal regulatory factor in adipogenesis.[39] FN-1, an ECM present during periods of change within tissues, exists in a functional form composed of fibers that are highly interwoven.[39] FN-1 is the key ECM protein that defines cell shape and contractility in close association with COL-1.[45,46] In adipocytes or adipose tissues, the expression of COL-1, COL-4, COL-6, and FN-1 and their alteration during adipogenesis were reported.[47,48] In fact, previous studies using a 2D culture of 3T3-L1 preadipocytes revealed in vitro remodeling from COL-1 and FN-rich ECM in undifferentiated cells into basement membrane-rich ECMs (e.g., COL-4) in differentiated cells.[43] In our current study, we used 3D HOF organoids to confirm that, upon adipogenic differentiation, downregulation of COL-1 and FN-1 and upregulation of COL-4 and COL-6 expression occur, which had been determined using 2D cell cultures as described previously.[47] With regard to the effect of PG analogs on 3D HOF organoids, adipogenesis-induced changes in ECM expression were significantly modulated, as described above, although the lipid proliferation during adipogenesis was not affected. It is well known that adipocytes in a 3D environment are supposed to be surrounded by a number of ECM proteins that constitute interstitial fibers and pericellular basement membranes.[30,49] Among these, if COL-1, the major ECM protein that provides the framework necessary to sustain the ECM structure, and its association with other ECMs, such as COL-6 and FN-1, were altered by the presence of PG analogs, then that would explain our observation of the significantly smaller sizes of the 3D HOF organoids without any change in lipid metabolism. In fact, it was previously reported that PGF2α facilitates pulmonary fibrosis through the FP receptor in a murine bleomycin-induced pulmonary fibrosis model in which the promoter activity of COL-1 was enhanced.[50–52]

In conclusion, our newly developed 3D cell culture of HOFs provided us with a better understanding of the molecular etiology of DUES by PG analogs, and its treatment and prevention using this methodology will be our subsequent project.

Acknowledgments

The authors specially thank Tae-Hwa Chun (Division of Metabolism, Endocrinology & Diabetes, Department of Internal Medicine, Biointerfaces Institute, University of Michigan) for his excellent technical advice of adipose tissue culture.

Disclosure: **K. Itoh**, None; **F. Hikage**, None; **Y. Ida**, None; **H. Ohguro**, None

References

1. Quigley HA, Broman AT. The number of people with glaucoma worldwide in 2010 and 2020. *Br J Ophthalmol*. 2006;90:262–267.
2. Schulzer M, Alward W, Feldman F, et al. Comparison of glaucomatous progression between untreated patients with normal-tension glaucoma and patients with therapeutically reduced intraocular pressures. *Am J Ophthalmol*. 1998;126:487–497.
3. Smid SD. Role of prostaglandins and specific place in therapy of bimatoprost in the treatment of elevated intraocular pressure and ocular hypertension: a closer look at the agonist properties of bimatoprost and the prostamides. *Clin Ophthalmol*. 2009;3:663–670.
4. Liton PB, Luna C, Challa P, Epstein DL, Gonzalez P. Genome-wide expression profile of human trabecular meshwork cultured cells, nonglaucomatous and primary open angle glaucoma tissue. *Mol Vis*. 2006;12:774–790.
5. Wiggs JL, Pasquale LR. Genetics of glaucoma. *Hum Mol Genet*. 2017;26:R21–R27.
6. Cheng JW, Cai JP, Wei RL. Meta-analysis of medical intervention for normal tension glaucoma. *Ophthalmology*. 2009;116:1243–1249.
7. Kass MA, Heuer DK, Higginbotham EJ, et al. The Ocular Hypertension Treatment Study: a randomized trial determines that topical ocular hypotensive medication delays or prevents the onset of primary open-angle glaucoma. *Arch Ophthalmol*. 2002;120:701–713; discussion 829–730.
8. Mackenzie P, Cioffi G. How does lowering of intraocular pressure protect the optic nerve? *Surv Ophthalmol*. 2008;53(suppl 1):S39–S43.
9. AGIS Investigators. The Advanced Glaucoma Intervention Study (AGIS): 7. The relationship between control of intraocular pressure and visual field deterioration. *Am J Ophthalmology*. 2000;130:429–440.
10. European Glaucoma Society. European Glaucoma Society Terminology and Guidelines for Glaucoma, 4th Edition - Chapter 3: Treatment principles and options supported by the EGS Foundation: Part 1: Foreword; Introduction; Glossary; Chapter 3 Treatment principles and options. *Br J Ophthalmol*. 2017;101:130–195.
11. Alm A. Latanoprost in the treatment of glaucoma. *Clin Ophthalmol*. 2014;8:1967–1985.
12. Ota T, Aihara M, Narumiya S, Araie M. The effects of prostaglandin analogues on IOP in prostanoid FP-receptor-deficient mice. *Invest Ophthalmol Vis Sci*. 2005;46:4159–4163.
13. Alm A, Grierson I, Shields MB. Side effects associated with prostaglandin analog therapy. *Surv Ophthalmol*. 2008;53(suppl 1):S93–S105.
14. Shah M, Lee G, Lefebvre DR, et al. A cross-sectional survey of the association between bilateral topical prostaglandin analogue use and ocular adnexal features. *PLoS One*. 2013;8:e61638.
15. Nakakura S, Terao E, Nagatomi N, et al. Cross-sectional study of the association between a deepening of the upper eyelid sulcus-like appearance and wide-open eyes. *PLoS One*. 2014;9:e96249.
16. Maruyama K, Tsuchisaka A, Sakamoto J, Shirato S, Goto H. Incidence of deepening of upper eyelid sulcus after topical use of tafluprost ophthalmic solution in Japanese patients. *Clin Ophthalmol*. 2013;7:1441–1446.
17. Aihara M, Shirato S, Sakata R. Incidence of deepening of the upper eyelid sulcus after switching from latanoprost to bimatoprost. *Jpn J Ophthalmol*. 2011;55:600–604.
18. Peplinski LS, Albiani Smith K. Deepening of lid sulcus from topical bimatoprost therapy. *Optom Vision Sci*. 2004;81:574–577.
19. Sakata R, Shirato S, Miyata K, Aihara M. Incidence of deepening of the upper eyelid sulcus in prostaglandin-associated periorbitopathy with a latanoprost ophthalmic solution. *Eye (Lond)*. 2014;28:1446–1451.
20. Park J, Cho HK, Moon JI. Changes to upper eyelid orbital fat from use of topical bimatoprost, travoprost, and latanoprost. *Jpn J Ophthalmol*. 2011;55:22–27.
21. Inoue K, Shiokawa M, Wakakura M, Tomita G. Deepening of the upper eyelid sulcus caused by 5 types of prostaglandin analogs. *J Glaucoma*. 2013;22:626–631.
22. Jayaprakasam A, Ghazi-Nouri S. Periorbital fat atrophy - an unfamiliar side effect of prostaglandin analogues. *Orbit*. 2010;29:357–359.
23. Kershaw EE, Flier JS. Adipose tissue as an endocrine organ. *J Clin Endocrinol Metab*. 2004;89:2548–2556.
24. Gregoire FM, Smas CM, Sul HS. Understanding adipocyte differentiation. *Physiol Rev*. 1998;78:783–809.
25. Evans RM, Barish GD, Wang YX. PPARs and the complex journey to obesity. *Nat Med*. 2004;10:355–361.
26. Taketani Y, Yamagishi R, Fujishiro T, Igarashi M, Sakata R, Aihara M. Activation of the prostanoid FP receptor inhibits adipogenesis leading to deepening of the upper eyelid sulcus in prostaglandin-associated periorbitopathy. *Invest Ophthalmol Vis Sci*. 2014;55:1269–1276.
27. Choi HY, Lee JE, Lee JW, Park HJ, Lee JE, Jung JH. In vitro study of antiadipogenic profile of latanoprost, travoprost, bimatoprost, and tafluprost in human orbital preadiopocytes. *J Ocul Pharmacol Ther*. 2012;28:146–152.
28. Beningo KA, Dembo M, Wang YL. Responses of fibroblasts to anchorage of dorsal extracellular matrix receptors. *Proc Natl Acad Sci U S A*. 2004;101:18024–18029.
29. Cukierman E, Pankov R, Yamada KM. Cell interactions with three-dimensional matrices. *Curr Opin Cell Biol*. 2002;14:633–639.
30. Chun TH, Hotary KB, Sabeh F, Saltiel AR, Allen ED, Weiss SJ. A pericellular collagenase directs the 3-dimensional development of white adipose tissue. *Cell*. 2006;125:577–591.
31. Huh D, Hamilton GA, Ingber DE. From 3D cell culture to organs-on-chips. *Trends Cell Biol*. 2011;21:745–754.
32. Hikage F, Atkins S, Kahana A, Smith TJ, Chun TH. HIF2A-LOX pathway promotes fibrotic tissue remodeling in thyroid-associated orbitopathy. *Endocrinology*. 2019;160:20–35.
33. Mori S, Kiuchi S, Ouchi A, Hase T, Murase T. Characteristic expression of extracellular matrix in subcutaneous adipose tissue development and adipogenesis; comparison with visceral adipose tissue. *Int J Biol Sci*. 2014;10:825–833.
34. Seibold LK, Ammar DA, Kahook MY. Acute effects of glaucoma medications and benzalkonium chloride on preadipocyte proliferation and adipocyte cytotoxicity in vitro. *Curr Eye Res*. 2013;38:70–74.
35. Chen J, Senior J, Marshall K, et al. Studies using isolated uterine and other preparations show bimatoprost and prostanoid FP agonists have different activity profiles. *Br J Pharmacol*. 2005;144:493–501.
36. Choi CJ, Tao W, Doddapaneni R, et al. The effect of prostaglandin analogue bimatoprost on thyroid-associated orbitopathy. *Invest Ophthalmol Vis Sci*. 2018;59:5912–5923.
37. Xiong H, Wu M, Zou H, et al. Chitosan inhibits inflammation and adipogenesis of orbital fibroblasts in Graves ophthalmopathy. *Mol Vis*. 2018;24:509–517.
38. Perumal S, Antipova O, Orgel JP. Collagen fibril architecture, domain organization, and triple-helical conformation govern its proteolysis. *Proc Natl Acad Sci USA*. 2008;105:2824–2829.

Investigative Ophthalmology & Visual Science

39. Chun TH. Peri-adipocyte ECM remodeling in obesity and adipose tissue fibrosis. *Adipocyte*. 2012;1:89–95.
40. Ricard-Blum S. The collagen family. *Cold Spring Harb Perspect Biol*. 2011;3:a004978.
41. Varma S, Orgel JP, Schieber JD. Nanomechanics of type I collagen. *Biophys J*. 2016;111:50–56.
42. Mak KM, Mei R. Basement membrane type IV collagen and laminin: an overview of their biology and value as fibrosis biomarkers of liver disease. *Anat Rec (Hoboken)*. 2017;300:1371–1390.
43. Aratani Y, Kitagawa Y. Enhanced synthesis and secretion of type IV collagen and entactin during adipose conversion of 3T3-L1 cells and production of unorthodox laminin complex. *J Biol Chem*. 1988;263:16163–16169.
44. Liu C, Huang K, Li G, et al. Ascorbic acid promotes 3T3-L1 cells adipogenesis by attenuating ERK signaling to upregulate the collagen VI. *Nutr Metab (Lond)*. 2017;14:79.
45. Spiegelman BM, Ginty CA. Fibronectin modulation of cell shape and lipogenic gene expression in 3T3-adipocytes. *Cell*. 1983;35:657–666.
46. Sottile J, Hocking DC. Fibronectin polymerization regulates the composition and stability of extracellular matrix fibrils and cell-matrix adhesions. *Mol Biol Cell*. 2002;13:3546–3559.
47. Kim B, Choi KM, Yim HS, Lee MG. Ascorbic acid enhances adipogenesis of 3T3-L1 murine preadipocyte through differential expression of collagens. *Lipids Health Dis*. 2013;12:182.
48. Nakajima I, Muroya S, Tanabe R, Chikuni K. Extracellular matrix development during differentiation into adipocytes with a unique increase in type V and VI collagen. *Biol Cell*. 2002;94:197–203.
49. Lijnen HR, Maquoi E, Demeulemeester D, Van Hoef B, Collen D. Modulation of fibrinolytic and gelatinolytic activity during adipose tissue development in a mouse model of nutritionally induced obesity. *Thromb Haemost*. 2002;88:345–353.
50. Aihara K, Handa T, Oga T, et al. Clinical relevance of plasma prostaglandin F2alpha metabolite concentrations in patients with idiopathic pulmonary fibrosis. *PLoS One*. 2013;8:e66017.
51. Oga T, Matsuoka T, Yao C, et al. Prostaglandin F(2alpha) receptor signaling facilitates bleomycin-induced pulmonary fibrosis independently of transforming growth factor-beta. *Nat Med*. 2009;15:1426–1430.
52. Olman MA. Beyond TGF-beta: a prostaglandin promotes fibrosis. *Nat Med*. 2009;15:1360–1361.